Fundamental Study of Coupling Methods between Energy Simulation and CFD

Tatsuhiro Yamamoto[1], Akihito Ozaki[2], Myongyang Lee[2],Hideki Kusumoto
[1]Graduate Student, Kyushu University, Hukuoka, Japan, yamamoto.t.313@s.kyushu-u.ac.jp
[2]Professor,Ph.D., Kyushu University, ozaki@arch.kyushu-.ac.jp
[3]Associate Prof, Ritsumeikan University, myonglee@ fc.ritsumei.ac.jp
[4] Graduate Student, Kyushu University, Hukuoka, Japan, 2he16409@s.kyushu-u.ac.jp

Abstract

We have developed a new coupling method between ES (energy simulation) and CFD (computational fluid dynamics). First, the validity of the coupling method in the stationary part is verified, and the temperature distribution of the space is predicted. At this time, we compare whether it is better to use a temperature boundary for the high boundary conditions or a heat flow boundary. An ES cannot consider the spatial temperature distribution, but it is possible to divide the space into any number of divisions. Since the amount of advection of the cross section of the space of the divided analysis model is not known, the temperature distribution of the space can be reproduced, even by ES, by integrating the values calculated by CFD. In this study, we clarify that the temperature distribution in an environment where natural convection by floor heating is dominant can be reproduced in detail by a combination of ES and CFD. We also conduct a fundamental study of a method for predicting the temperature of an arbitrarily divided zone in a large space. As a result, the temperature distribution when the amount of advection is coupled is clarified.

Introduction

Numerical simulation in a modern architectural environment is roughly divided into ES (energy simulation) and CFD (computational fluid dynamics). Since ES is a single mass model, it is possible to consider a long-term nonstationary analysis. However, CFD is not suitable for a nonstationary analysis because of the large calculation load, but it can reproduce the properties of a distribution, such as the temperature and wind speed of a cross section in detail. A coupling method has been proposed that couples the process from the CFD to the convective heat transfer coefficient from the ES by converging the surface temperature calculated from the ES as a boundary condition (Zhai et al. 2002) From a method for calculating the convective heat transfer coefficient by ES, the accuracy of the convective heat transfer coefficient from the ES becomes questionable when analyzing a local space that has a cooling/heating surface (Zhai et al. 2004). The convective heat transfer coefficient of ES typified by TRNSYS uses a fixed value, and there is some doubt about the degree. THERB for HAM(Simulation Software of the Thermal Environment of Residential Building for Heat and Mass Transfer) is an ES that calculates the Nusselt numbers along the indoor floor surface, wall surface, outer wall, and convection heat transfer coefficient. However, we use Rayleigh number to calculate the Nusselt number on the interior side. Therefore, a positive value cannot be calculated in the case of an airflow field with a Reynolds number greater than a certain number, as in convection and in the case of a large temperature difference. Therefore, CFD can accurately calculate the convective heat transfer coefficient. From this background, coupling ES with CFD is indispensable for obtaining a practical space–temperature distribution to understand specific physical phenomena in detail. In addition, a method for linking the heat transfer including the latent heat transfer and the amount of advection calculated from CFD has not yet been established. Therefore, in this research, the conditions for coupling are clarified, a new coupling method is established, and a database of coupling conditions is constructed. The temperature distribution of the space where natural convection is dominant, as represented by floor heating in the coupling, is elucidated from the viewpoint of the coupling with ES. ES and the verification of the actual measurement accuracy have been carried out in the past for the purpose of investigating the indoor thermal environment of a hot-water floor heating system (Lee et al. 2016) The boundary condition calculated by the steady-state ES was used in the CFD, and a convergence calculation was carried out to reproduce the cross-sectional distribution of the actual measurement value and confirm the validity of the coupling.

In recent years, houses built in metropolitan areas cannot escape from the narrowing trend accompanied by the increase in land prices, and the open ceiling space is reviewed from its openness and continuity. To grasp the thermal environment in a large space, investigations using CFD are mainly performed (Yuki et al. 2014); however, a long-term nonstationary analysis using ES has not been conducted. An unsteady analysis is required at the time of design, but it is difficult to carry out in a large space such as an atrium. The reason for this is that when analyzing large spaces by ES, it is necessary to divide the large space into arbitrary zones; thus, the amount of advection between each zone is unknown, and the accuracy of the calculation is questionable. Therefore, when analyzing large spaces, it is difficult to calculate the heat quantity of an arbitrarily divided zone by only ES. However, the distribution of the input heat quantity in each zone may be provided by CFD. Calculation load is low because CFD only performed steady analysis once.

Outline of the methodology by coupling

Outline of the dynamic thermal load calculation software THERB

In this research, the ES uses THERB for HAM, which is dynamic thermal load calculation software. THERB can predict the thermal moisture and air movement of an architectural system strictly according to physical phenomena concerning conduction, convection, and radiation; the heat load; and the thermal environment of many rooms. The spatial temperature, humidity, and heat load according to the time and period are calculated using the weather conditions, building model, and life schedule as input conditions, similar to ES.

All phenomena are calculated without simplification of the heat and moisture transfer principles of any building components or elements. The moisture transfer model using the water potential, which is defined as the thermodynamic energy, is a progressive feature and incorporates moisture transfer including the moisture sorption and desorption for walls. Thus, THERB can predict the hygrothermal environment of the entire building considering the complex relationship between the heat and moisture transfer and the airflow. (Ozaki et al. 2006)

Time-varying convective heat transfer coefficient

In an environment where natural convection is dominant, it is possible to calculate the convective heat transfer coefficient by using boundary-layer theory (profile method) or a dimensionless formula based on an experimental law (Fujii et al. 1972, Ozaki et al. 1990). The natural convection heat transfer coefficient is calculated using the dimensionless equations expressed in Eqs. (1)–(5). The Nusselt number is a dimensionless number determined by the Rayleigh number. In general, the Rayleigh number in a turbulent flow region is in the range of 109–1015. THERB calculates both the forced and natural convection for each of the inner and outer surfaces and each part of the air layer.

[Horizontal plane]

$$Nu = C \cdot Ra_f^m \tag{1}$$

$$Ra_f = Gr_i \cdot \Pr \tag{2}$$

$$f = (T_s + T_\infty)/2 \tag{3}$$

[Vertical surface]

$$Nu = 0.241(Gr_i \cdot \Pr) \tag{4}$$

$$Gr_i = g\beta\Delta T_a l^3 / v_2 \tag{5}$$

The coefficient C and exponent m in Eq. (1) are as follows:

[Upward heat flow]

$C = 0.58 \quad m = 1/5$

[Downward heat flow]

$C = 0.54 \quad m = 1/4 \quad (Ra_f : 2\times10^4 - 8\times10^6)$

$C = 0.15 \quad m = 1/3 \quad (Ra_f : 8\times10^6 - 1\times10^{11})$

The convective heat transfer coefficient α_c is expressed as follows for a flat plate using the Nusselt number Nu and representative length:

$$\alpha_c = \frac{Nu \cdot \lambda}{l} \tag{6}$$

Hot-water-piping floor heating system

The finite difference method is applied to the model of the one-dimensional transient hygrothermal conduction of multilayered walls (part of THERB). Regarding the thermal conduction to the ground, a two- or three-dimensional finite difference method is applied to the previous calculation of the ground temperature; then, the results are used as the input excitation for the conduction calculation of the earthen floor and basement walls.

The fin efficiency, which explains the ratio of the actual heat transfer from the fin surfaces to the hypothetical heat transfer assuming that the fin temperature is equal to the hot-water temperature in a tube, is applied to the hydronic floor heating system.

The following equations are used to calculate the fin efficiency:

[Fin efficiency]

$$\eta_f = \frac{1}{w}[D + (w - D)\frac{\tanh \cdot mD}{mD}] \tag{7}$$

$$mD = \sqrt{\frac{C_f \cdot P}{\lambda_f \cdot t}} D \tag{8}$$

[Heat transmission coefficient from hot water to the tube surface]

$$K_p = \frac{A_f}{L_f \cdot R_b} \tag{9}$$

$$R_b = \frac{D}{\lambda_w \cdot Nu} \tag{10}$$

$$Nu = \frac{0.0395 \cdot Re^{0.75} \cdot Pr}{1.0 + (1.99 \cdot Re^{-0.125} \cdot (Pr - 1.0))} \tag{11}$$

[Heat balance for hot water]

$$C_w \cdot \rho_w \cdot V_w \frac{\partial T}{\partial t} = \eta_f \cdot K_p \cdot (T_m - T_w) \cdot L_f + Q_s \tag{12}$$

$$Q_s = q_f \cdot C_w \cdot \rho_w (T_{ws} - T_w) \tag{13}$$

$$\begin{aligned} -\frac{\partial T}{\partial t} &= \eta_f \cdot K_p (T_m - T_w) \\ &= \frac{1}{R_m}(T_m - T_{m-1}) + \frac{1}{R_{m+1}}(T_m - T_{m+1}) \end{aligned} \tag{14}$$

Calculation of the heat transfer coefficient by CFD

An ES calculates the convective heat transfer coefficient based on boundary-layer theory and experimental laws. Although the theory adopted in the ES has an extremely high precision, the temperature of the zone is used; thus, the influence of the distribution cannot be taken into account. In CFD, it is possible to consider the anisotropy of the turbulence in each cell. Based on this

characteristic, there is an advantage by the condition depending on the CFD calculation. The case in which the convective heat transfer coefficient can be calculated with CFD is expressed by Eq. (15). As shown in Figure 2, the reference temperature is set as the first cell of the surface (t_{wall}) or at an arbitrary Y^+ position (t_{fluid}). There are other methods to set the reference temperature and to calculate the natural convection heat transfer coefficient. In this analysis, the calculation method that can consider a three-dimensional flow field and a reference with Y^+ that can refer to the temperature of the turbulent flow region is adopted.

$$h_{wall} = \frac{q_{wall}}{(t_{wall} - t_{fluid})} \quad (15)$$

Coupling overview

Figures 1 and 2 show the coupling flowchart and method. There are several types of coupling, and there are several suggested ones. For simplicity, there is one-step coupling that only gives the boundary conditions obtained by ES to CFD and two-step coupling that returns the boundary conditions from CFD to ES. In this analysis, the surface temperature (t_{wall}) obtained by ES is given as the boundary condition of CFD, and the convective heat transfer coefficient (h_{wall}) is transferred from CFD and coupled until the convergence condition (the difference in the surface temperature) is satisfied. At the same time step (t), dynamic coupling is adopted. The physical quantities to be released from ES to CFD are the surface temperature and heat flow.

Heated floor heating analysis of natural convection control

A database of the indoor thermal environments at the time of heating use is insufficient. An unsteady analysis by ES at the time of floor heating use is possible, but there is no prior research from the point of view of reproducing the cross-sectional distribution by CFD at the time of coupling. Mathieu et al. (2014) verified the accuracy of the temperature at the measurement point in the height direction, but the distribution was not reproduced. In this analysis, the temperature distribution at steady state is reproduced.

Experimental surveys are conducted in an environment where natural convection is excellent, and the accuracy is verified by an unsteady analysis using THERB. The THERB result after 8 h of the rise in the stationary part is 24.97 °C, which reasonably agrees with the measured value of 25.34 °C. In this analysis, we compare the spatial distribution due to coupling with CFD at the stationary part (after 8 h).

Outlines of the experiment and calculation

Figures 3 and 4 show an outline and section of the experimental building. The experiment is carried out in a one-story experimental building wing installed in the test room. The room to be measured in the experiment was set as room A. The outer shape of room A is 3.6 m (x) × 3.6 m (y) × 2.6 (z), and the floor area is 12.96 m^2 (8 tatami). The installation rate of hot-water mats is 70% (8.17 m×) of the floor area. The heat insulation performance is equivalent to the new energy saving standard (1992 standard). The pipe diameter is 0.0098 m, and the pitch is 0.075 m. The temperature in the environmental test room was set to be constant at 5 °C, and floor heating in room A operated for 8 hours. The temperature and hot-water flow rate were measured during operation. The air temperature was measured at 150 points in room A, 1 point in room B, 1 corner, and 1

Figure 1 Coupling flowchart

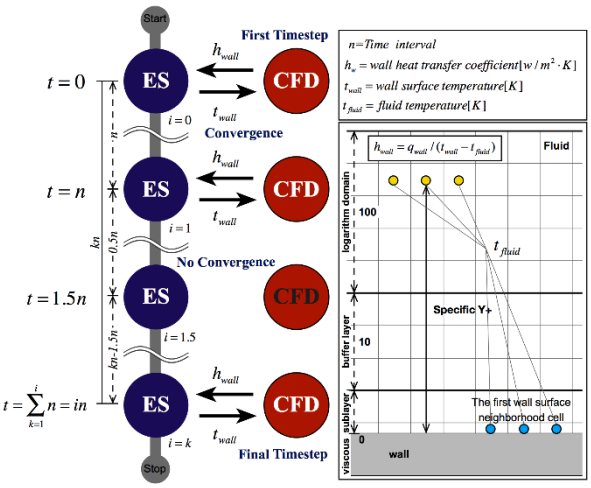

Figure 2 Coupling method and reference temperature concept

location underneath the floor.

Conditions for CFD analysis

The CFD analysis model is shown in Figure 5 The boundary conditions of the CFD are listed in Table 1. The calculation area has the same outline as room A in the experimental building. Since the convection heat transfer coefficient is determined at the time of coupling, handling near the wall is extremely important; therefore, the vicinity of the wall was sufficiently resolved as being less than $Y^+ > 1$. The standard k–ε low-Reynolds-number-type turbulent flow model was adopted, which can reproduce the thermal environment near the wall. In this analysis, the input heat quantity when hot water is continuously operated for 8 h is integrated from one hour before, and the average value is taken as the boundary condition of the CFD. Figure 6 shows the temperature boundary conditions. The convection heat transfer coefficient is large because the heat flow is large at the heat generation surface.

Results of the numerical calculation

Figures 7 and 8 show the bulk temperature analysis results. The ES calculation results are supplemented with accurate measurements, but when coupled with the boundary condition of the ES to the CFD, the room temperature calculated by the CFD was 25.27 °C, which is closer to the actual measurement result. In the distribution of the cross section(b-b and c-c), the temperature in the lower part of the central part is locally high owing to advection from the lower-left part and a cold draft from the window surface. It is thought that this is because the advection direction of natural convection changed owing to the effect of modeling the draft wind in the CFD. The upper-left temperature of the a-a cross section is higher because the advection by the cold draft and the draft wind are combined Because it is only natural convection, it is thought that it was delicately influenced by the draft wind because the wind speed is low.

Coupled analysis of advection using ES and CFD

The actual phenomena of natural and forced convection are presented when reproducing the temperature distribution of a large space. That is, the analysis method for the reproduction of the temperature distribution in a large space is different owing to the introduction of an air conditioner. In the coupled analysis we will conduct basic studies for the purpose of developing an analysis method for the temperature distribution of a large space in the presence of natural convection under solar irradiation and forced convection with the introduction of an air conditioner.

Solar radiation with multiple reflections between indoor surfaces

THERB is superior for calculating the sunlit and shadowed sides compared with other ESs. A brief description using mathematical expressions is as follows. TDN_m [W/m^2] is the direct solar radiation entering the

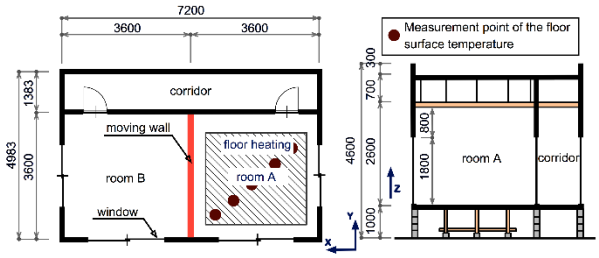

Figure 3 Outline of the experimental building

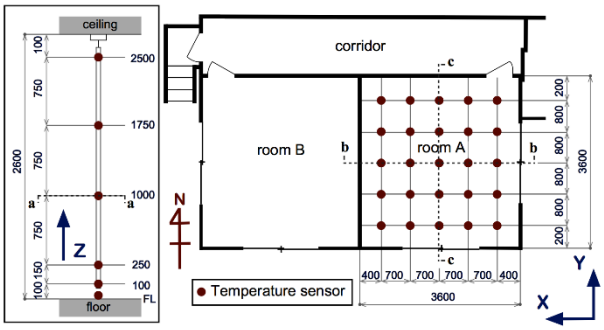

Figure 4 Air temperature measurement points

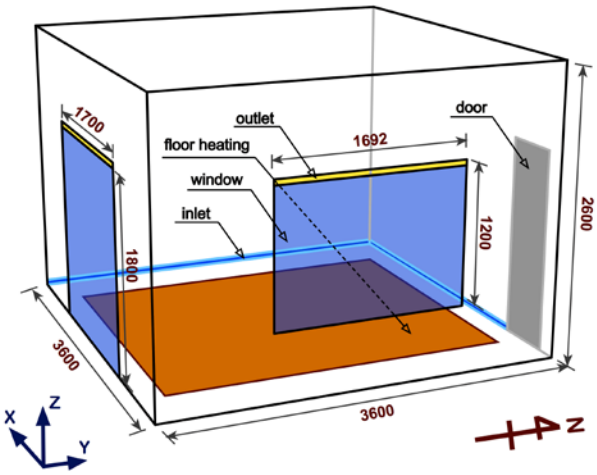

Figure 5 CFD analysis model

Table 1 CFD analysis conditions

item	Boundary conditions
Calculation area	3.6m(x)×3.6(y)×2.6m(z)
Computational lattice	2,392,170
Turbulence model	Standard K - ε low Reynolds number
Inflow entrance	Pressure outlet：0[Pa] temperature：278.15[K]
Outflow outlet	Flow distribution outlet：0.1回/h
Floor heating input heat quantity	The average value from 1 hour before the analysis target time according to Expressions (12) to (14)（1189.462W）
Window / Wall / Door	According to the examination case of Figure 6

interior surface *m* through the window surface. The solar absorption rate and solar reflectance of the surface *1*, the incident angle with respect to the surface *l*, and the sunlit area of the surface *l* are taken as direct solar radiation. The amounts of solar radiation absorbed by and reflected

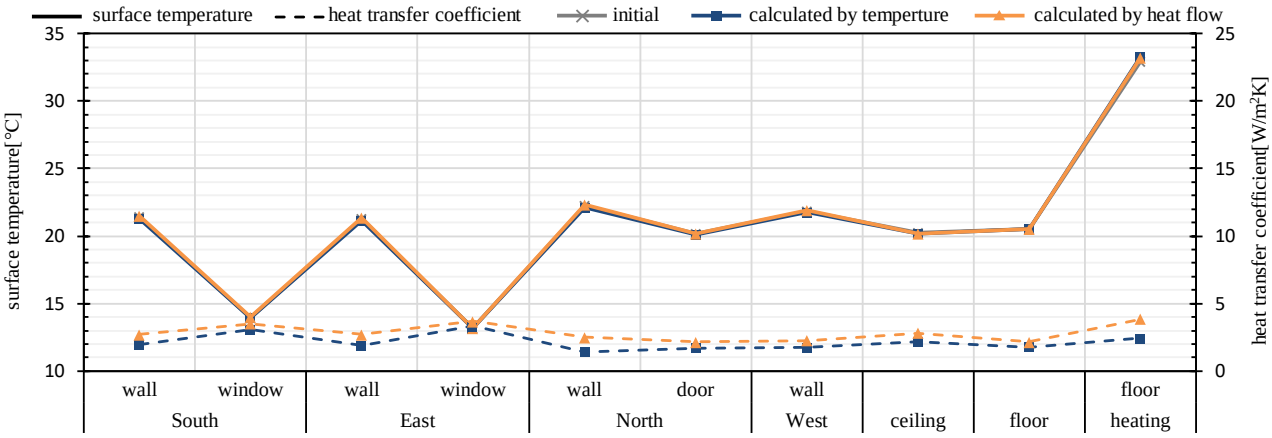

Figure 6 Temperature boundary conditions

from the inner surface *1* due to the primary incidence are represented by and respectively. Therefore, the amount of solar radiation absorbed by the net inner surface *j*, $ADT_{m,j}$ [W/m^2], is expressed by Eq. (17) using TDN_m and the short-wave absorption coefficient in Eq. (16).

$$\gamma_{l,j} = F_{l,j}a_j + \sum_{k=1}^{J} F_{l,k}\rho_k\gamma_{k,j} \tag{16}$$

$$ADT_{m,j} = TDN_m \sum_{l=1}^{L} \left(\delta_{j,l}a_l \cos\theta_l + \rho_l\gamma_{l,j}\cos\theta_l S_l/S_j\right) \tag{17}$$

(when $j = l$, $\delta_{j,l} = 1$; when $j \neq l$, $\delta_{j,l} = 0$)

Using the reciprocity theorem in Eq. (18), Eq. (17) can be expressed as shown in Eq. (19).

$$a_l S_l \gamma_{l,j} = a_j S_j \gamma_{j,l} \tag{18}$$

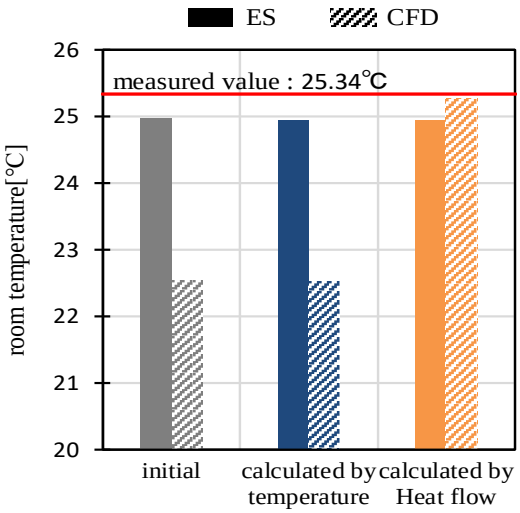

Figure 7 Bulk temperature analysis results

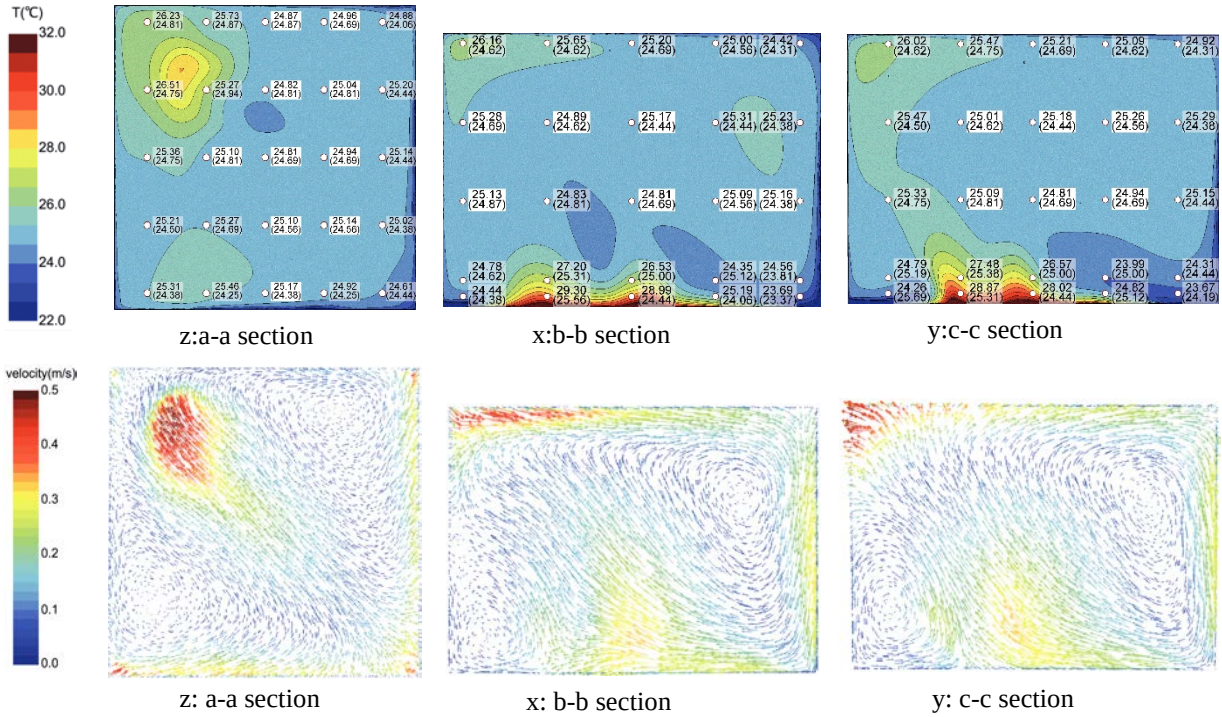

Figure 8 Bulk temperature analysis results (upper: temperature, lower: velocity)

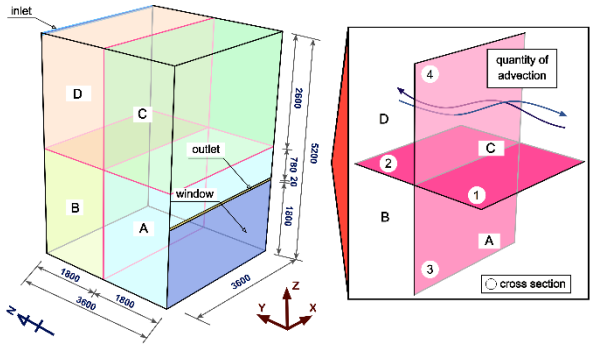

Figure 9 Transfer flow analysis model

$$ADT_{m,j} = a_j \cdot TDN_m \sum_{l=1}^{L} \left(\delta_{j,l} + \rho_l \gamma_{j,l} / a_l\right) \cos\theta_l \qquad (19)$$

When ADW_m [W/m^2] represents the direct solar radiation absorption of window m (indoor side glass in the case of double glazing), the amount of solar radiation absorbed by the inner surface j, ADT_j [W/m^2], can be obtained by

$$ADT_j = \sum_{m=1}^{M} \left\{ \delta_{j,m} ADW_m + a_j \cdot TDN_m \sum_{l=1}^{L} \left(\delta_{j,l} + \rho_l \gamma_{j,l} / a_l\right) \cos\theta_l \right\} \qquad (20)$$

Let TSD_m [W/m^2] be the diffused solar transmittance of window m and ASW_m [W/m^2] be the window m. Assuming the amount of diffused solar radiation absorption and that TSD_m [W/m^2] diffuses evenly into the room, the amount of solar radiation absorbed by the inner surface j, AST_j [W/m^2], due to the diffused solar radiation is given by

$$AST_j = \sum_{m=1}^{M} \left(\delta_{j,m} ASW_m + a_j \gamma_{j,m} TSD_m / a_m\right) \qquad (21)$$

Therefore, the net amount of short-wave radiant heat absorbed by the inner surface j, NLR_j [W/m^2], is obtained by

$$NSR_j = ADT_j + AST_j \qquad (22)$$

Calorimetric calculation of sunlight

The amount of heat given as a boundary condition to be input into the CFD is only the amount of convection. In this analysis, the amount of convective heat transfer is calculated by THERB and used as a boundary condition for CFD. Assuming that the amount of convective heat transfer from the surface is CV_j [W], the amount of long-wave radiation heat absorbed and radiated from the wall surface is NLR_j [W], and the amount of wall heat transfer is CD_j [W]. Further, the amount of short-wave radiation absorbed and incident on the wall surface is NSR_j [W] and expressed as

$$NSR_j = CV_j + NLR_j + CD_j \qquad (23)$$

By rearranging Eq. (23), CV_j can be obtained using

Table 2 Review case and wall structure

Wall configuration(Inside→Outside)　　( )thickness [mm]

	Case-1	Case-2	Case-3
Roof	Plywood 12 Plywood 12	Plywood 12 Glass wool 40 Plywood 12	Adiabatic
South			
North			
East	Adiabatic	Adiabatic	
West			
Floor	Plywood(12)+XPS(12)+Plywood(12)+Adiabatic		

Table 3 THERB calculation conditions

Date and time	January 9 12:00 (Winter)
area	Tokyo
Weather	Expanded AMeDAS weather data（Standard year）
air conditioning	No air conditioning
Preliminary calculation	7days
Calculation time interval	10minutes
Transfer flow rate	initial:20times convergenced:According to Table 6

$$CV_j = NSR_j - NLR_j - CD_j \qquad (24)$$

Here, the amount of heat transfer is expressed as

$$CD_j = \frac{\lambda}{l}(T_{j,s} - T_{j,i}) A_j \qquad (25)$$

THERB analysis conditions

Table 2 summarizes the THERB study case and wall structure. In this analysis, for the purpose of generating a circulating flow and inputting the amount of advection into THERB, the east and west sides are insulated, and the wall structures of the roof, south, and north surfaces are changed. Further, a sensitivity analysis was performed. The window is 3 mm single glass. Wall 2 is used as a reference, and 40-mm-thick glass wool is introduced and verified on Wall 1 without insulation and an adiabatic boundary. Table 3 summarizes the analysis conditions of THERB.

CFD analysis conditions

The boundary conditions of the transfer flow CFD are listed in Table 4, and the CFD analysis model is shown in Figure 9. The calculation area is 3.6 m (x) × 3.6 m (y) × 5.2 m (z), which is the outline obtained by adding the upper blow through to the plane scale of the analysis model of theFigure6. The ventilation system introduces a third system that pulls by ventilation 0.5 times at the inlet The inflow temperature was taken as the outside air temperature. The CFD boundary conditions and analysis results are listed in Figure 10. The heat flow calculated using Eqs. (23)–(25) is given to the floor of room A, which is a sunlit surface.

Analysis results

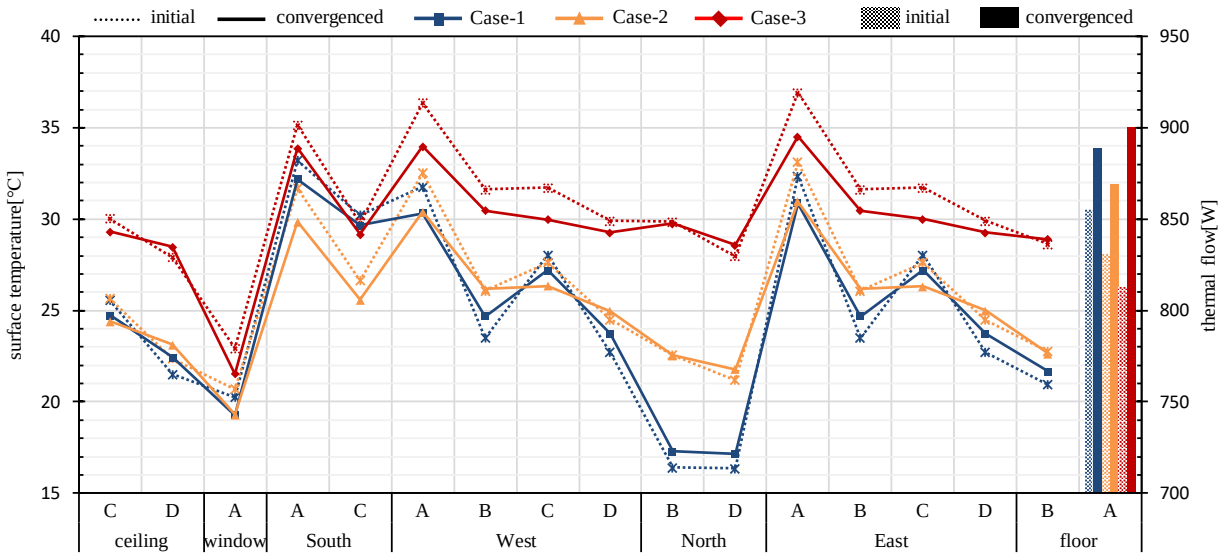

Figure 10 Wall and floor boundary conditions

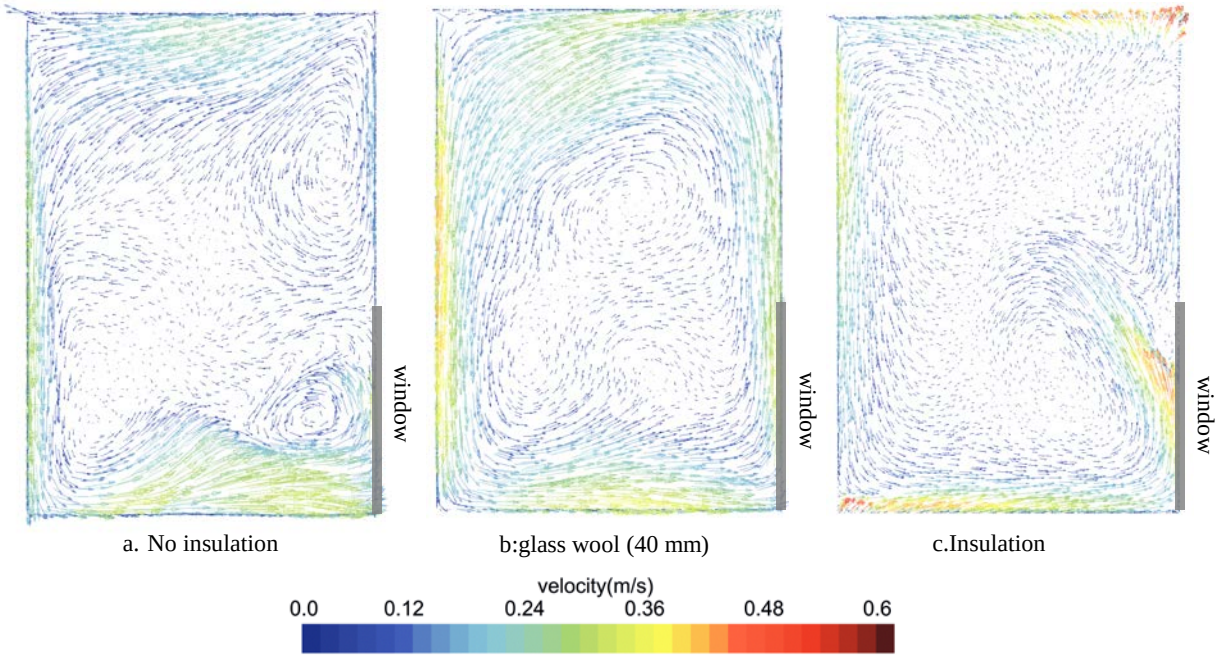

a. No insulation b:glass wool (40 mm) c.Insulation

Figure 11 Transfer-flow-coupled analysis results (x = 1800)

Table 5 summarizes the calculation results for the amount of advection, and Figure 11 shows the transfer-flow-coupled analysis results. From Figure 11, it can be seen that a circulating flow is generated. The wind speed is large for no insulation < glass wool < insulation. From the analysis results in Figures 12 and 13, the temperature tends to be higher in the order of A > C > D > B, which is the direction of advection in which a circulating flow occurs. After coupling, the temperature difference between the upper and lower parts decreases, and the

Table 4 CFD analysis conditions

item	Boundary conditions
Calculation area	3.6m(x)×3.6m(y)×5.2m(z)
Computational lattice	2,106,749
Turbulence model	Standard K - ε low Reynolds number
Inflow entrance	Pressure outlet：0[Pa] temperature：279.05[K]
Outflow outlet	Flow inlet：0.5times/h temperature：281.55[K]
Heat input surface	Equations (8) to (9) and Table 1
Wall / window surface	According to the analysis case of Figure10

Table 5 Transfer flow analysis results

(m^3/h)

cross section	Case-1	Case-2	Case-3
1	1774.1	2459.5	1972.7
2	1818.4	2458.3	2012.0
3	1809.6	2493.1	2008.1
4	1818.4	2457.0	1971.8

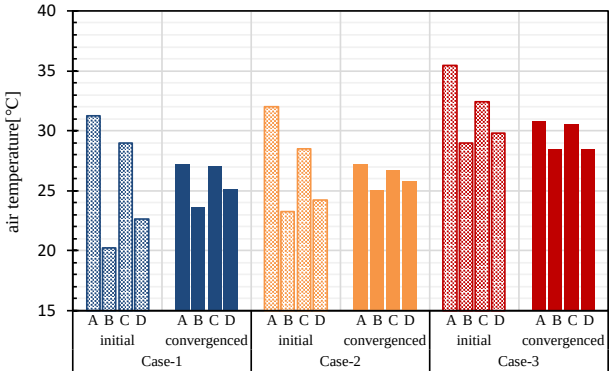

Figure 12 Room temperature for each case

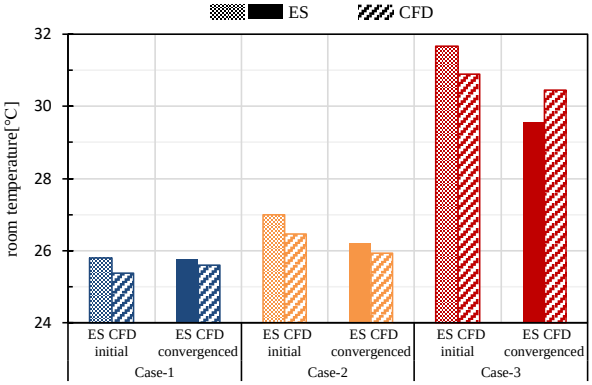

Figure 13 Bulk temperature for each case

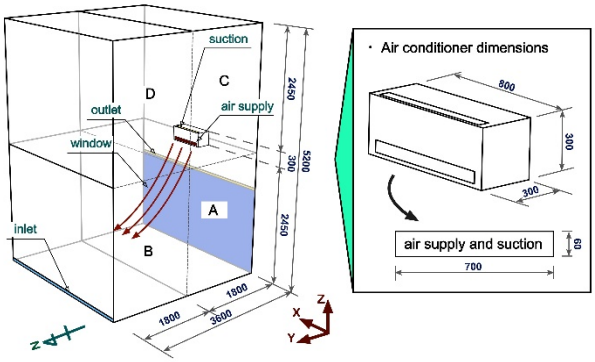

Figure 14 CFD analysis model

Table 7 Transfer flow analysis results

(m^3/h)

cross section	1	2	3	4
Transfer flow	6917.2	7617.9	7572.6	7614.6

temperature of room A, which contains the sunlit surface, decreases as heat moves by advection. Figure 10 shows the boundary conditions between the wall and the floor. The quantity of heat radiated upon the floor is higher after coupling. It is thought that this is because CD_j and NLR_j decrease as the surface temperature decreases. By linking the transfer flow rates, the temperature in each space decreases and affects the surface temperature. The bulk temperature generally agrees with THERB and CFD, and the difference after coupling is small. Moreover, the coupling accuracy is high. The bulk temperature tends to be low after coupling, but this is accompanied by a decrease in the surface temperature.

Coupled analysis of the heat input to a fan-powered unit heater and the amount of advection

The coupling air conditioning and CFD is mainly conducted for offices (Shiraisi et al. 2011). However, an air-conditioning calculator is not a zone model but mainly air-conditioning simulation software such as the LCEM tool and HVACSIM + (J). Further, it is not done in a zone model such as THERB or TRNSYS. As a fundamental study of the coupling of a fan-powered unit heater and CFD, by introducing the sensible heat load

Table 6 THERB calculation conditions

Date and time	January 9 22:00 (Winter)
area	Tokyo
Weather	Expanded AMeDAS weather data (Standard year)
air conditioning	Heating the room A up to 20℃
Preliminary calculation	7days
Calculation time interval	10minutes
Transfer flow rate	According to Table 8

calculated by CFD to the optional air-conditioning target area of the ES and combining the flow rates, we introduced a fan-powered unit heater on the ES side. The analysis was carried out with the aim of calculating the temperature distribution of a space when introducing air conditioner .

THERB analysis conditions

Table 7 summarizes the analysis conditions of THERB for air-conditioner coupling. We calculated the nighttime that needed heating.

CFD analysis conditions

The CFD boundary conditions are the same as those in Table 4. This analysis was carried out according to the following procedure.

① Set A to 20 °C as the boundary condition of ES and calculate the boundary condition (surface temperature) of CFD.

② Calculate the air-conditioning set temperature so that the it becomes 20 °C and analyze the CFD with the surface temperature of ① as the boundary condition.

③ Analyze the transfer result, the quantity of heat, and the convection heat transfer coefficient, which are the analysis results of ② as the conditions for setting the ES. The amount of heat is given to A.

④ CFD is analyzed with the surface temperature and the amount of heating (used for the calculation of the air-conditioning set temperature) as the boundary conditions, which are the analysis results of ③.

The air-conditioning load is calculated by multiplying the CFD blowing temperature and suction temperature by the specific heat and specific weight.

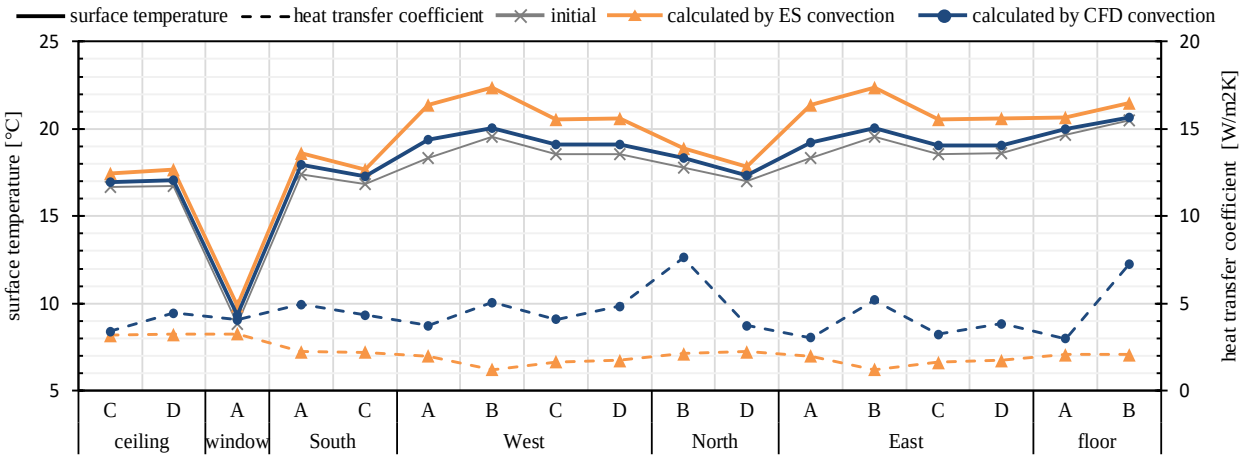

Figure 15 Wall boundary conditions and convective heat transfer coefficient

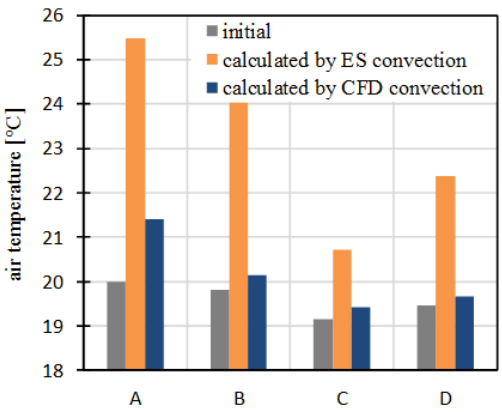

Figure 16 Each room temperature

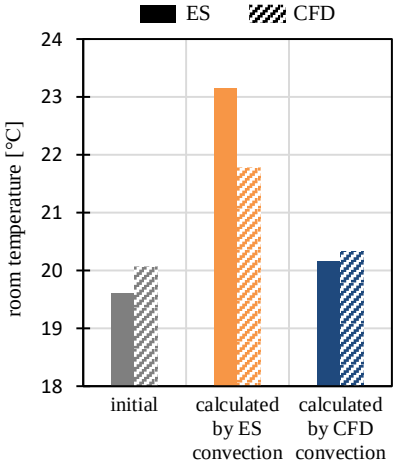

Figure 17 Bulk temperature analysis results

The airflow of the fan-powered unit heater was set at a flow rate of 12 m^3/min, and the temperature was 30 °C for the first time and 33.21 °C for the second time(④). Figure 14 shows the CFD analysis model at the time of coupling with the fan-powered unit heater. The outer shape is the same as that for the amount of transfer coupling. An air supply port is installed at the lower part because it becomes a factor that hinders the generation of a circulating flow by forced convection. The amount of heat input into THERB is the value obtained by multiplying the suction temperature and blowing temperature by the specific heat and specific gravity.

Analysis results

The results for the amount of advection are shown in Figures 15–17. Owing to the forced convection due to the introduction of a fan-powered unit heater, a large amount of ventilation is obtained as compared with the analysis of natural convection. The examination section(x=1800) of advection was assumed to be equivalent to that in Figure 9. Figure 18 shows the wind speed distribution. A circulating flow of 3 → 2 → 4 → 1(cross section) is formed by the advection of the fan-powered unit heater. As a result of coupling with the same boundary conditions, the bulk temperatures of THERB and CFD have a high correlation with a 0.1 ℃ difference; thus, the coupling accuracy is high. The bulk temperature of each chamber is higher in the order of A > B > D > C and is the same as the advection direction.

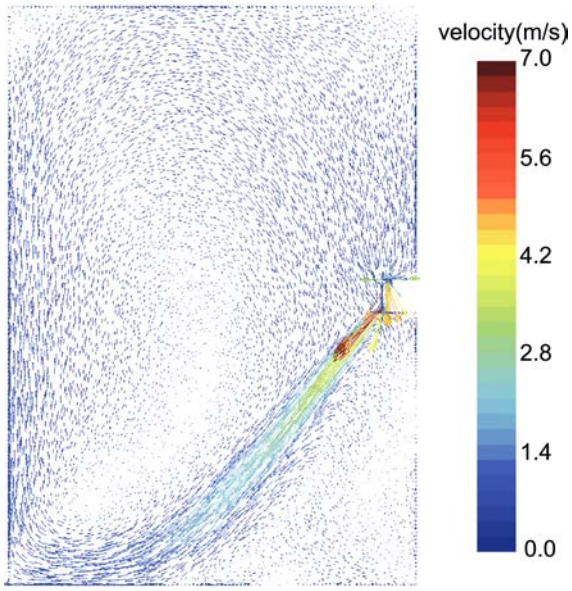

Figure 18 Wind speed distribution (x = 1800)

The convective heat transfer coefficient calculated by THERB is lower than the calculated value of the CFD, and the bulk temperature tends to increase because the temperature estimate was high owing to the influence of the heat loss. Since the bulk temperature is almost the same value when the calculated CFD values are used, it is considered that the convective heat transfer coefficient of THERB tends to be underestimated in the forced convection environment.

Conclusion

In this research, we confirmed the accuracy of a coupled analysis in the natural state and expanded it to couple the amount of advection. In addition, we conducted a fundamental study so that the correct room temperature can be calculated in the zone model by coupling a fan-powered unit heater with the zone model.(1) It is possible to reproduce the temperature distribution of the space by steady state synchronous in an environment where natural convection is dominant. (2) Calculation of the sunlit surface, accurate reproduction of the boundary conditions, and linking the amount of advection indicate that the temperature of each zone due to heat diffusion can be predicted by an ES.(3) It was confirmed that the temperature distribution of a large space with the introduction of the air conditioner could be predicted by joining the amounts of advection and input heat. During forced convection, it is found that the bulk temperature matches by connecting the convective heat transfer coefficient.

Nomenclature

A_f : internal area of tube [m^2]
C_f : thermal conductance from fin surface [$W/(m^2.K)$]
C_w : specific heat of water [J/(kg.K)]
D : diameter of tube [m]
F : view factor [-]
Gr : Grashof number [-]
K_p : apparent turbulent heat transfer coefficient in tube [$W/(m^2.K)$]
L_f : length of tube [m]
LI_c, LH_f : radiant heat from lights and appliances and human bodies [-]
Nu : Nusselt number [-]
P : circumferential length of tube [m] Pr : Prandtle number [-]
Q_s : amount of heat [W]
R_b : thermal resistance per unit length from inner surface to outer surface of tube[m^2.K/W]
R_m : thermal resistance of material [m^2.K/W]
Ra : Rayleigh number [-]
Re : Reynolds number [-]
T_M : mean temperature of surfaces [K]
T_m : temperature in floor [K]
T_s : supply hot-water temperature [K]
T_w : temperature in tube [K]
ΔT_a: temperature difference between surface and air [K]
ΔT_s: temperature difference between surfaces [K]
Q_s : amount of heat [W]
V_w : amount of water [m^3]
g : gravitational constant [=9.8 m/s^2]
l : characteristic length [m]
q_f : flow rate of hot-water [m^3/s]
t : thickness of tube [m]
v : kinematic viscosity [m^2/s]
w : pitch of tube [m]
h_{wall} :convection heat transfer coefficient of wall surface [$W/(m^2 \cdot K)$]
q_{wall} :heat flux on wall [W/m^2]
t_{wall} :wall surface temperature [K]
t_{fluid} :fluid temperature [K]

Reference

Heinz R. Trechsel 2001. Moisture Analysis and Condensation Control in Building Envelopes, American Society for Testing and Materials,

MNL40Ozaki A., Watanabe T. et al. 2001, Systematic Analysis on Combined Heat and Water Transfer through Porous Materials Based on Thermodynamic Energy, Journal of Energy and Buildings, Vol.33, No.4, p.341-350

Zhai Z, Chen Q,other 2002. On approaches to couple energy simulation and computational fluid dynamics programs, Building and Environment, Vol.37,pp.857-864

Zhai Z, Chen Q 2004. Performance of coupled building energy and CFD simulation, Energy and Buildings, Vol37, pp333-344

Shiraishi Y,Shinohara N,Maehara K.Sagara N 2011. Study on HVAC −system −performance Simulator Based on Coupled Simulation of HVAC System Simulation and CFD Analysis Proceeding of society of heating,Air-conditioning Sanitary Engineere of Japan,No.176,pp.19-26

Fujii W. and Imura H. 1972, Natural Convection Heat Transfer from a Plate with Arbitrary Inclination, Int. J. Heat Mass Transfer, Vol.15, p.755-767

Ozaki A., Watanabe T. et al. 2001, Systematic Analysis on Combined Heat and Water Transfer through Porous Materials Based on Thermodynamic Energy, Journal of Energy and Buildings, Vol.33, No.4, p.341-350

Yuki T et al. 2014.Study on Thermal and Air Environment Control in an Atrium Space covered with Glass Curtain Walls Verification of HVAC Control System according to Zone in Summer and Winter by CFD Analysis. Architectural Institute of Japan Summary Academic Lecture Collection Summary. pp.1291-129

LEE M et al.2016.Analysis of an Indoor Environmet With aHydronic Floor-Heating System Under the Sensory Index.J.Environ Eng.AIJ.Vol.81.No.719.pp.65-71

Mathieu B, Sigrid R 2014. Coupling building energy simulation and computational fluid dynamics: Application to a two-storey house in a temperate climate. Building and Environment, Vol.75, pp.30

Rode C., Woloszyn M. 2009, Common Exercises in Whole Building HAM Modelling, Proc. of the 11th International IBPSA Conference, p.346-353